PHILOSOPHICAL MAGAZINE B, 1998, VOL. 77, NO. 3, 787–803

Green's function for electron scattering and its applications in low-voltage point-projection microscopy and optical potential

By Z. L. WANG†

School of Material Science and Engineering, Georgia Institute of Technology, Atlanta, Georgia 30332-0245 USA

[*Received 17 June 1997 and accepted 2 July 1997*]

ABSTRACT

The Green's function is a powerful mathematical tool in developing the theory of condensed-matter physics. It is usually easy to write the equation in the form of $G(\mathbf{r},\mathbf{r}')$, but the critical challenge is to find its analytical or numerical solution. In this paper, the Green's function for electron scattering is reviewed, and its general solution is given. The theory is extended into the regimes that are suitable for numerical calculations in different scattering geometries, such as the images in the low-voltage lensless point-projection microscopy. An iterative calculation technique is introduced for computing the Green's function using the Born series, and the result is applied to calculate the optical potential introduced in electron diffraction for recovering the multiple diffuse scattering effects. With the Green's function presented here and the theory reported previously by Wang (1996, *Phil. Mag.* B, **74**, 733), quantitative analysis of electron diffuse scattering due to short-range order of point defects and thermal diffuse scattering is likely to be feasible.

§ 1. INTRODUCTION

The Green's function, as a powerful tool in mathematical physics, plays a vital role in developing many theories in condensed-matter and particle physics. Using the Green's function, the Schrödinger equation can be transformed from its differential form into an integral form, allowing introduction of the perturbation theory and iterative calculation. The books by Abrikosov *et al.* (1963) and Tsvelick (1995) have systematically summarized the general characteristics of the Green's function. For dynamic electron scattering in crystalline materials and surfaces containing point defects, the full calculation of the diffraction intensity requires the solution of the Green's function (Wang 1996a, b).

Diffuse scattering in electron diffraction can be produced by time-dependent thermal vibration of crystal atoms and/or disordered or partially ordered spatial distribution of point defects, such as vacancies and interstitials. The growth of thin films in molecular-beam epitaxy is a typical example of a partially ordered system. The growth of the surface layer is a time-dependent process depending on the deposition rate and the diffusion rate of the surface atoms. This layer-by-layer growth is qualitatively described by a surface coverage parameter θ, with $0 \leqslant \theta \leqslant 1$, which represents the probability that a lattice site on the surface is filled with an atom. The sites unfilled with atoms are vacancies. Electron scattering from this

† e-mail: zhong.wang@mse.gatech.edu.

system needs to be approached using the Green's function theory (Dundarev *et al.* 1993, 1994). It has been rigorously proven (Wang 1996b, c) that, by inclusion of a complex optical potential V' in dynamic calculation, the dynamic multiple diffuse scattering due to point defects is fully included although the calculation is performed using the equation derived under the distorted-wave Born approximation (DWBA). This conclusion expands the applications of the existing theories for electron diffraction in a partially ordered system, but the key here is to find the solution of the Green's function that is required for computing the optical potential. It is generally easy to write equations in the form of the Green's function; the real challenge is how to get the solution of the equation that can be used directly for numerical calculations.

As a continuation of the previous report (Wang 1996c), this paper is intended to review the general solution of the Green's function and to develop it into the formats that are required in practical calculations for different electron scattering geometry. In § 2 the general solution of the Green's function is given. The limiting cases of the general solution for several special cases, such as the image in low-voltage lensless poing-projection microscopy (Fink *et al.* 1991, Spence *et al.* 1993), will be given in § 3. In § 4 an interactive method for calculating the Green's function using the Born series is introduced. Finally, § 5 gives the calculation of the optical potential V'. The theory outlined in this paper is for both low- and high-energy electrons.

§ 2. Formal solution of the Green's function

As a general approach to electron scattering, the electron source function is represented by $S(\mathbf{r})$ which characterizes the intensity distribution and size of the source (fig. 1). The electron energy is E which is related to its wave-vector $\mathbf{K}_0$ by $E = (h^2K_0^2)/(2m_0)$, where m_0 is the electron mass. If the inelastic scattering is ignored, the scattering behaviour of the electron is governed by the Schrödinger equation

$$\left(-\frac{\hbar^2}{2m_0}\nabla^2 - e\gamma V_0(\mathbf{r}) - E(K_0) \right) \Psi(\mathbf{r}) = S(\mathbf{r}), \tag{1}$$

where $V_0(\mathbf{r})$ is a periodic structurally averaged crystal potential that is responsible for the dynamic Bragg reflections (Wang 1996c), and $\gamma = 1/(1 - v^2/c^2)^{1/2}$ stands for the relativistic correction. The electron source function can be written as an integral of point sources characterized by the Dirac delta functions $\delta(\mathbf{r} - \mathbf{r}')$:

$$S(\mathbf{r}) = \int \mathrm{d}\mathbf{r}' S(\mathbf{r}')\delta(\mathbf{r} - \mathbf{r}'). \tag{2a}$$

Similarly, the wavefunction is written as a superposition of the waves generated by point sources $\delta(\mathbf{r} - \mathbf{r}')$ (e.g. the Green's function $G(\mathbf{r}, \mathbf{r}')$), centred at $\mathbf{r}'$ and weighted by the intensity of the source at $\mathbf{r}'$:

$$\Psi(\mathbf{r}) = \int \mathrm{d}\mathbf{r}' S(\mathbf{r}')G(\mathbf{r}, \mathbf{r}'). \tag{2b}$$

Substituting eqns. (2*a*) and (2*b*) into eqn. (1) yields

$$\left(-\frac{\hbar^2}{2m_0}\nabla^2 - e\gamma V_0(\mathbf{r}) - E(K_0) \right) G(\mathbf{r}, \mathbf{r}') = \delta(\mathbf{r} - \mathbf{r}'). \tag{3}$$

Fig. 1

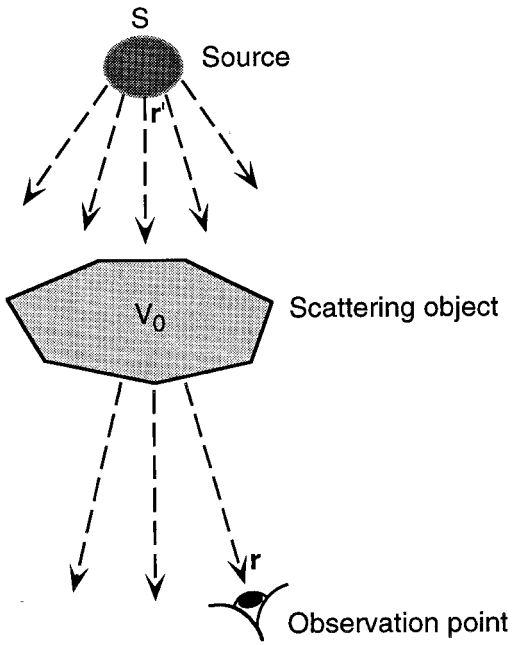

Electrons emitted from a finite source S are scattered by a local potential V_0, and the observation point is at $\mathbf{r}$.

This is the equation that determines the Green's function. The solution of eqn. (3) has been given under the small-angle scattering approximation for the zeroth-order Laue zone reflections (Wang 1995a, § 10.5). Here we outline the solution given by Dudarev *et al.* (1994) for a general case without making any approximation. The details are repeated here for the convenience of discussions in later sections.

The solution is based on the Born series with an assumption that the series converges. This assumption holds for the known condensed matter that one is interested in. By shifting the EG term to the right-hand side in eqn. (3) and using the Green's function in vacuum as the zeroth-order solution G_0 (e.g. taking $V_0 = 0$) which satisfies

$$\left(-\frac{\hbar^2}{2m_0}\nabla^2 - E(K_0) \right) G_0(\mathbf{r},\mathbf{r}') = \delta(\mathbf{r} - \mathbf{r}') \tag{4a}$$

and has the solution

$$G_0(\mathbf{r},\mathbf{r}') = \frac{2m_0}{\hbar^2}\frac{\exp(2\pi i K_0|\mathbf{r} - \mathbf{r}'|)}{4\pi|\mathbf{r} - \mathbf{r}'|} = \frac{m_0}{2\pi^2\hbar^2}\int d\boldsymbol{\kappa}\,\frac{\exp[2\pi i\boldsymbol{\kappa}\cdot(\mathbf{r} - \mathbf{r}')]}{\kappa^2 - K_0^2 - i0}, \tag{4b}$$

where 0 stands for an infinite small but positive number, the general solution of

eqn. (3) can be written as the Born series

$$\begin{aligned} G(\mathbf{r},\mathbf{r}') &= G_0(\mathbf{r},\mathbf{r}') + e\gamma \int d\mathbf{r}_1\, G_0(\mathbf{r},\mathbf{r}_1)\, V_0(\mathbf{r}_1) G(\mathbf{r}_1,\mathbf{r}') \\ &= G_0(\mathbf{r},\mathbf{r}') + e\gamma \int d\mathbf{r}_1\, G_0(\mathbf{r},\mathbf{r}_1)\, V_0(\mathbf{r}_1) G_0(\mathbf{r}_1,\mathbf{r}') \\ &\quad + (e\gamma)^2 \int d\mathbf{r}_1 \int d\mathbf{r}_2\, G_0(\mathbf{r},\mathbf{r}_1) G_0(\mathbf{r}_1,\mathbf{r}_2)\, V_0(\mathbf{r}_1)\, V_0(\mathbf{r}_2) G_0(\mathbf{r}_2,\mathbf{r}') \\ &\quad + (e\gamma)^3 \int d\mathbf{r}_1 \int d\mathbf{r}_2 \int d\mathbf{r}_3\, G_0(\mathbf{r},\mathbf{r}_1) G_0(\mathbf{r}_1,\mathbf{r}_2) G_0(\mathbf{r}_2,\mathbf{r}_3)\, V_0(\mathbf{r}_1) \\ &\quad \times V_0(\mathbf{r}_2)\, V_0(\mathbf{r}_3) G_0(\mathbf{r}_3,\mathbf{r}') + \cdots . \end{aligned} \tag{5}$$

From the expression given in eqn. (4*b*), the Green's function is a superposition of plane waves whose amplitudes depend on the energy of the plane-wave component. This indicates that one may write the general solution of the Green's function in a similar form. This approach can be further developed with consideration of the scattering of a plane wave, $\phi(\boldsymbol{\kappa},\mathbf{r}) = \exp(2\pi i \boldsymbol{\kappa}\cdot\mathbf{r})$, by the crystal potential, which is determined by the Schrödinger equation

$$\left(-\frac{\hbar^2}{2m_0}\nabla^2 - E(\kappa) \right) \Psi_0^{(0)}(\mathbf{K},\mathbf{r}) = e\gamma\, V_0(\mathbf{r})\, \Psi_0^{(0)}(\mathbf{K},\mathbf{r}). \tag{6}$$

The solution of eqn. (6) for high-energy electron scattering can be solved using a variety of existing theories, as reviewed elsewhere (Wang 1995a). The iterative solution of $\Psi_0^{(0)}$ is

$$\begin{aligned} \Psi_0^{(0)}(\boldsymbol{\kappa},\mathbf{r}) &= \phi(\boldsymbol{\kappa},\mathbf{r}) + e\gamma \int d\mathbf{r}_1\, G_0(\mathbf{r},\mathbf{r}_1)\, V_0(\mathbf{r}_1)\, \Psi_0^{(0)}(\boldsymbol{\kappa},\mathbf{r}_1) \\ &= \phi(\boldsymbol{\kappa},\mathbf{r}) + e\gamma \int d\mathbf{r}_1\, G_0(\mathbf{r},\mathbf{r}_1)\, V_0(\mathbf{r}_1) \phi(\boldsymbol{\kappa},\mathbf{r}_1) \\ &\quad + (e\gamma)^2 \int d\mathbf{r}_1 \int d\mathbf{r}_2\, G_0(\mathbf{r},\mathbf{r}_1) G_0(\mathbf{r}_1,\mathbf{r}_2)\, V_0(\mathbf{r}_1)\, V_0(\mathbf{r}_2) \phi(\boldsymbol{\kappa},\mathbf{r}_2) \\ &\quad + (e\gamma)^3 \int d\mathbf{r}_1 \int d\mathbf{r}_2 \int d\mathbf{r}_3\, G_0(\mathbf{r},\mathbf{r}_1) G_0(\mathbf{r}_1,\mathbf{r}_2) G_0(\mathbf{r}_2,\mathbf{r}_3) \\ &\quad \times V_0(\mathbf{r}_1)\, V_0(\mathbf{r}_2)\, V_0(\mathbf{r}_3) \phi(\boldsymbol{\kappa},\mathbf{r}_3) + \cdots . \end{aligned} \tag{7}$$

We now go back to the general solution of the Green's function. Substituting the last G_0 in each term of eqn. (5) by the integral form of G_0 given in eqn. (4*b*), while the other G_0 are kept the same, eqn. (5) becomes

$$\begin{aligned} G(\mathbf{r},\mathbf{r}') = \frac{C}{\pi} \int d\boldsymbol{\kappa}\, \frac{\exp(-2\pi i \boldsymbol{\kappa}\cdot\mathbf{r}')}{\kappa^2 - K_0^2 - i0} \Bigg(& \phi(\boldsymbol{\kappa},\mathbf{r}) + e\gamma \int d\mathbf{r}_1\, G_0(\mathbf{r},\mathbf{r}_1)\, V_0(\mathbf{r}_1) \phi(\boldsymbol{\kappa},\mathbf{r}_1) \\ & + (e\gamma)^2 \int d\mathbf{r}_1 \int d\mathbf{r}_2\, G_0(\mathbf{r},\mathbf{r}_1) G_0(\mathbf{r}_1,\mathbf{r}_2)\, V_0(\mathbf{r}_1)\, V_0(\mathbf{r}_2) \phi(\boldsymbol{\kappa},\mathbf{r}_2) \\ & + (e\gamma)^3 \int d\mathbf{r}_1 \int d\mathbf{r}_2 \int d\mathbf{r}_3\, G_0(\mathbf{r},\mathbf{r}_1) G_0(\mathbf{r}_1,\mathbf{r}_2) G_0(\mathbf{r}_2,\mathbf{r}_3) \\ & \times V_0(\mathbf{r}_1)\, V_0(\mathbf{r}_2)\, V_0(\mathbf{r}_3) \phi(\boldsymbol{\kappa},\mathbf{r}_3) + \cdots \Bigg), \end{aligned} \tag{8}$$

where $C = m_0/(2\pi\hbar^2)$. A comparison of the terms inside the large parentheses in eqn. (8) with eqn. (7) leads to

$$G(\mathbf{r},\mathbf{r}') = \frac{C}{\pi}\int d\boldsymbol{\kappa}\,\frac{\exp(-2\pi i\boldsymbol{\kappa}\cdot\mathbf{r}')}{(\kappa^2 - K_0^2 - i0)}\,\Psi_0^{(0)}(\boldsymbol{\kappa},\mathbf{r}). \tag{9}$$

This is a key relation that correlates the Green's function with the solution of the Schrödinger equation for an incident plane wave of wave-vector $\boldsymbol{\kappa}$. Using an identity

$$\int d\mathbf{u}\,\frac{\exp\left[2\pi i\mathbf{u}\cdot(\mathbf{r}'' - \mathbf{r}')\right]}{\pi(u^2 - K_0^2 - i0)} = \frac{\exp\left[2\pi i K_0|\mathbf{r}'' - \mathbf{r}'|\right]}{|\mathbf{r}'' - \mathbf{r}'|}, \tag{10 a}$$

or

$$\frac{\exp(-2\pi i\boldsymbol{\kappa}\cdot\mathbf{r}')}{\pi(\kappa^2 - K_0^2 - i0)} = \int d\mathbf{r}''\exp(-2\pi i\boldsymbol{\kappa}\cdot\mathbf{r}'')\,\frac{\exp(2\pi i K_0|\mathbf{r}'' - \mathbf{r}'|)}{|\mathbf{r}'' - \mathbf{r}'|}, \tag{10 b}$$

the Green's function can be written in a different form

$$G(\mathbf{r},\mathbf{r}') = C\int d\mathbf{r}''\,\frac{\exp(2\pi i K_0|\mathbf{r}' - \mathbf{r}''|)}{|\mathbf{r}' - \mathbf{r}''|}\left(\int d\boldsymbol{\kappa}\exp(-2\pi i\boldsymbol{\kappa}\cdot\mathbf{r}'')\,\Psi_0^{(0)}(\boldsymbol{\kappa},\mathbf{r})\right). \tag{11 a}$$

It has been proven that the G function given by eqn. (11) satisfy the *reciprocity theorem* $G(\mathbf{r},\mathbf{r}') = G(\mathbf{r}',\mathbf{r})$ (see the appendix), which means that the wavefunction 'observed' at $\mathbf{r}$ due to a point source at $\mathbf{r}'$ is the same as the wavefunction at $\mathbf{r}'$ due to a point source at $\mathbf{r}$, which is

$$G(\mathbf{r},\mathbf{r}') = C\int d\mathbf{r}''\,\frac{\exp(2\pi i K_0|\mathbf{r} - \mathbf{r}''|)}{|\mathbf{r} - \mathbf{r}''|}\left(\int d\boldsymbol{\kappa}\exp(-2\pi i\boldsymbol{\kappa}\cdot\mathbf{r}'')\,\Psi_0^{(0)}(\boldsymbol{\kappa},\mathbf{r}')\right). \tag{11 b}$$

This is the exact expression for the Green's function for a general case. The most beautiful part of this solution is the exact relationship between the conventional solution of the Schrödinger equation for plane-wave incidence with the solution for point source, but the amount of numerical calculation is very large. The limiting cases of this general solution for several practical situations are given in the next section.

§ 3. Applications

3.1. *Imaging in low-voltage lensless point-projection microscopy*

We now consider the scattering geometry of the low-voltage lensless point-projection microscopy (figure 2 (*a*)), in which a point source is positioned in the front of the specimen and a low voltage (less than 400 V) is applied to the tip (Fink *et al.* 1991, Spence *et al.* 1993). The image is recorded at a plane that is far from the specimen and it is a 'projection' of the crystal structure superposed with Fresnel fringes. The image magnification is determined by the distance of the source to the specimen and the distance from the tip to the projection screen. The Born series form of the Green's function (eqn. (5)) has been applied by Kreuzer *et al.* (1992) to calculate the images with the use of the spherical harmonics expansion of the G_0 function. In this section, we outline the application of eqn. (11 *b*) for the calculation of this type of image.

In this scattering geometry with a magnification larger than 500 000×, we can assume that the observation point is located at large distances so that $r \gg r'$; thus

$$|\mathbf{r} - \mathbf{r}''| = (r^2 + r''^2 - 2\mathbf{r}\cdot\mathbf{r}'')^{1/2} \approx r - \frac{\mathbf{r}\cdot\mathbf{r}''}{r};$$

Fig. 2

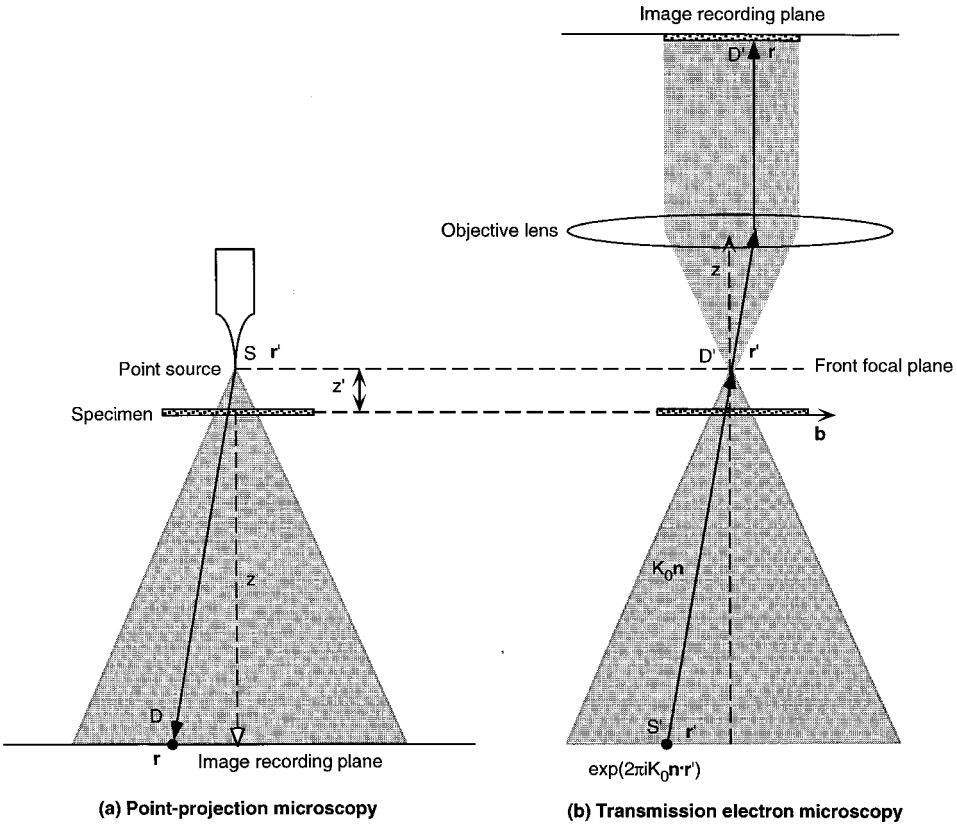

(*a*) The geometry of the low-voltage lensless point-projection microscopy, in which a thin specimen is illuminated by a point source S and the observation screen is located at a farther distance. The image magnificantion $M \approx z/z'$. (*b*) An equivalent image formation process in TEM, where the electron wavefunction at D′ due to an incident plane wave from S′ equals the wave observed at D owing to a point source at S. The image observed in point-projection microscopy is equivalent to the shadow image observed in large-angle convergent-beam TEM.

eqn. (11 *b*) is approximated as

$$G(\mathbf{r},\mathbf{r}') \approx C\frac{\exp(2\pi iK_0 r)}{r}\int d\mathbf{r}''\exp\left(-2\pi iK_0\frac{\mathbf{r}\cdot\mathbf{r}''}{r}\right)\left(\int d\boldsymbol{\kappa}\exp(-2\pi i\boldsymbol{\kappa}\cdot\mathbf{r}'')\,\Psi_0^{(0)}(\boldsymbol{\kappa},\mathbf{r}')\right)$$
$$= C\frac{\exp(2\pi iK_0 r)}{r}\,\Psi_0^{(0)}(\boldsymbol{\kappa}_r,\mathbf{r}'), \qquad (12)$$

where $\boldsymbol{\kappa}_r = -K_0(\mathbf{r}/r)$, antiparallel to $\mathbf{r}$. The image intensity observed at $\mathbf{r}$ for a point source located at $\mathbf{r}'$ is

$$I(\mathbf{r},\mathbf{r}') = |G(\mathbf{r},\mathbf{r}')|^2 = C^2\frac{|\Psi_0^{(0)}(\boldsymbol{\kappa}_r,\mathbf{r}')|^2}{r^2}, \qquad (13)$$

which means the intensity observed at $\mathbf{r}$ is the intensity observed at $\mathbf{r}'$ for an incident plane wave with a wave-vector $\boldsymbol{\kappa}_r$ antiparallel to $\mathbf{r}$. In other words, the wave observed at D (detector) when a point source is located at S (source) is equivalent to the wave observed at S due to an incident plane wave of wave-vector $\boldsymbol{\kappa}_r = -K_0(\mathbf{r}/r)$ from D. This is just the reciprocity theorem. The factor of $1/r^2$ represents the decay in the intensity of the spherical wave as the observation point moves away from the source. The observed intensity is scaled according to $\left|\Psi_0^{(0)}(\boldsymbol{\kappa}_r, \mathbf{r}')\right|^2$, which is the solution of the Schrödinger equation at $\mathbf{r}'$ for an incident plane wave with wave-vector $\boldsymbol{\kappa}_r$.

To illustrate the physical meaning of eqn. (12), an image formation process in transmission electron microscopy (TEM) following the form of the wavefunction $\Psi_0^{(0)}(\boldsymbol{\kappa}_r, \mathbf{r}')$ is given in fig. 2(*b*), in which a specimen is illuminated by a convergent beam and the specimen is located at z' below the front focal plane of the transmission electron microscope, with $z' \gg d$. Within the convergence cone, each incident beam direction is specified by a wave-vector $K_0\mathbf{n}$, where $\mathbf{n} = \mathbf{r}/r$ stands for the unit vector of position $\mathbf{r}$. This is the convergent beam shadow imaging in TEM with a defocus equal to the tip-to-specimen distance z' (Spence 1992). From the reciprocity theorem, the intensity observed at D′ due to an incident plane wave with wave-vector $K_0\mathbf{n}$ from S′ is the same as the intensity observed at point D due to a point source at S. From the mathematical relation given by eqn. (13), the image is equivalent to the bright-field image in scanning transmission electron microscopy (STEM), formed using a point detector positioned at the optic axis at D′ while a *plane wave* is rocked (or scanned) across the angular range of the cone convergence, in agreement with the conclusion of Spence and Qian (1992). Therefore the image calculation is similar to the simulation of STEM images with consideration the defocus z'. We now outline the formal dynamic theory for simulating this type of images.

For a thin crystal slab in the geometry given in fig. 2(*b*) illuminated by an incident plane wave $\exp(2\pi \mathrm{i} K\mathbf{n}\cdot\mathbf{r}')$, the transmitted wave at the exit face of the crystal is written in the Bloch wave form (Humphreys 1979)

$$\Psi_{c0}^{(0)} = \exp\left[2\pi \mathrm{i} K_0 \mathbf{n}\cdot\mathbf{r}'\right]\Phi_{c0}^{(0)} \tag{14a}$$

and

$$\Phi_{c0}^{(0)}(K_0\mathbf{n}, \mathbf{r}') = \sum_i \alpha_i(K_0\mathbf{n}) \sum_g C_g^{(i)}(K_0\mathbf{n}) \exp\left[2\pi \mathrm{i}\mathbf{g}\cdot\mathbf{b}' + 2\pi \mathrm{i}(g_z + \upsilon_i)d\right], \tag{14b}$$

where α_i are the superposition coefficients determined by the boundary conditions, $\mathbf{b}' = (x', y')$, $C_g^{(i)}$ are the Bloch wave coefficients determined by the eigenequation, and d is the specimen thickness. The numerical calculation of α_i and $C_g^{(i)}$ for low-energy electrons has been given by Qian *et al.* (1993).

The propagation of this wave from the exit face of the crystal to the front-focal plane is characterized by a convolution of the Fresnel propagator under the small-angle scattering approximation, thus the wave observed at the front focal plane (i.e. the D′ plane) of the objective lens is (Cowley 1995)

$$\Phi_0^{(0)}(K_0\mathbf{n}, \mathbf{r}') = \left[\Phi_{c0}^{(0)}(K_0\mathbf{n}, \mathbf{r}')\right] \otimes P(\mathbf{b}', z). \tag{15}$$

where $\otimes$ stands for the convolution calculation of $\mathbf{b}'$, and the propagation function for an inclined incidence is (Ishizuka 1982, Wang 1995a, § 3.2)

$$P(\mathbf{b}', z') = \frac{K_0}{\mathrm{i}z'} \exp\left[2\pi \mathrm{i} K_0(z' - \mathbf{n}\cdot\mathbf{r}')\right] \exp\left(\frac{\pi \mathrm{i} b'^2 K_0}{z'}\right). \tag{16}$$

If the cross-over point D′ is located at $\mathbf{r}' = (0, 0, z')$ the local electron wavefunction is given by

$$\Phi_0^{(0)}(K_0\mathbf{n}, \mathbf{r}')\big|_{\mathbf{b}'=0} = \exp\left[2\pi i K_0(1 - n_z)z'\right] \sum_i \alpha_i(K_0\mathbf{n}) \sum_g C_g^{(i)}(K_0\mathbf{n}) \exp\left[2\pi i(g_z + \upsilon_i)d\right] \times \exp\left(\frac{-\pi i\left[(K_0 n_x + g_x)^2 + (K_0 n_y + g_y)^2\right]z'}{K_0}\right). \quad (17)$$

If the objective lens is an ideal lens without aberration, the image intensity is given by

$$I(\mathbf{r}) = \frac{C^2}{r^2} \sum_i \sum_j \alpha_i(K_0\mathbf{n}) \alpha_j^*(K_0\mathbf{n}) \sum_g \sum_h C_g^{(i)}(K_0\mathbf{n}) C_h^{(j)*}(K_0\mathbf{n}) \times \exp\left[2\pi i(g_z - h_z + \upsilon_i - \upsilon_j)d\right] \times \exp\left(\frac{\pi i\left[(K_0 n_x + h_x)^2 + (K_0 n_y + h_y)^2 - (K_0 n_x + g_x)^2 - (K_0 n_y + g_y)^2\right]z'}{K_0}\right). \quad (18)$$

If the electron cross-over is at the specimen, for example $z' = 0$, eqn. (18) becomes

$$I(\mathbf{r}) = \frac{C^2}{r^2} \sum_i \sum_j \alpha_i(K_0\mathbf{n}) \alpha_j^*(K_0\mathbf{n}) \sum_g \sum_h C_g^{(i)}(K_0\mathbf{n}) C_h^{(j)*}(K_0\mathbf{n}) \times \exp\left[2\pi i(g_z - h_z + \upsilon_i - \upsilon_j)d\right], \quad (19)$$

which is the intensity distribution in the convergent-beam electron diffraction (CBED) pattern with disc overlap (Spence and Zuo 1992). The term contained in square brackets in eqn. (17) represents the defocus effect. Therefore the calculation is similar to the rocking surface in defocused CBED except the beam convergence is considerably larger than the Bragg angles.

3.2. *Plane-wave incidence in transmission electron microscopy*

In high-energy electron diffraction, the source is usually considered to locate at infinity from the specimen, for example $z' = -\infty$, but the observation point can be near the specimen, which is defined as the front focal plane of the objective lens in TEM. The wave emitted by the source is equivalent to a plane wave with wave-vector $\mathbf{K}_0$ when falls on the surface of the specimen (fig. 3), and the direction of $\mathbf{K}_0$ is antiparallel to $\mathbf{r}'$ and is determined by

$$K_{0x} = -\frac{x'}{r'} K_0, \quad K_{0y} = -\frac{y'}{r'} K_0, \quad K_{0z} = -\frac{z'}{r'} K_0 \quad (20)$$

if the origin is defined at the intersection of the optic axis with the crystal entrance surface. By assuming that $r' \gg r''$ in the integral of the Green function in eqn. (11 *a*), this yields

$$\left|\mathbf{r}' - \mathbf{r}''\right| = (r'^2 + r''^2 - 2\mathbf{r}' \cdot \mathbf{r}'')^{1/2} \approx r' - \frac{\mathbf{r}' \cdot \mathbf{r}''}{r'} = r' + \frac{\mathbf{K}_0 \cdot \mathbf{r}''}{K_0};$$

Fig. 3

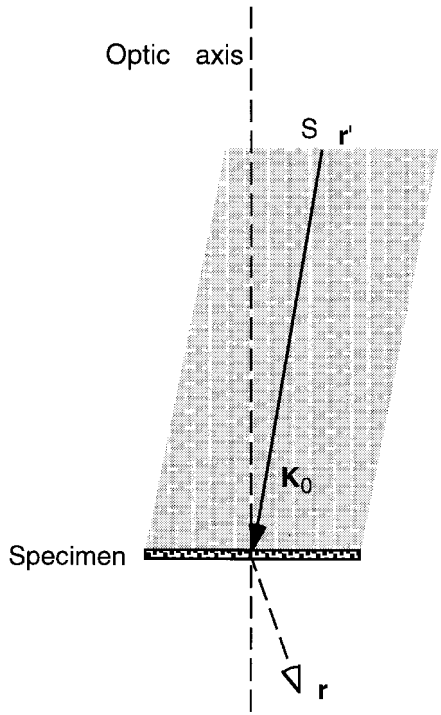

Scattering geometry for the electron source located at infinity.

thus

$$G(\mathbf{r},\mathbf{r}') \approx C\frac{\exp(2\pi i K_0 r')}{r'}\int d\mathbf{r}''\int d\kappa \exp(2\pi i\mathbf{K}_0\cdot\mathbf{r}'')\exp(2\pi i\kappa\cdot\mathbf{r}'')\,\Psi_0^{(0)}(-\kappa,\mathbf{r})$$

$$= C\frac{\exp(2\pi i K_0 r')}{r'}\,\Psi_0^{(0)}(\mathbf{K}_0,\mathbf{r}). \qquad (21)$$

where the spherical wave represents the wave emitted from the point source when it reaches the crystal surface, $\Psi_0^{(0)}(\mathbf{K}_0,\mathbf{r})$ is just the conventional elastic scattering wave arising from an incident plane wave with wave-vector $\mathbf{K}_0$. The observation point is usually chosen as the exit face of the crystal, which is defined as the front local plane of the objective lens. This is the basis of TEM imaging.

3.3. *Point source convergent-beam diffraction*

In dynamic calculation for diffuse scattering in high-energy electron scattering and under the DWBA, a two-dimensional Fourier transform of the Green's function is needed. This calculation can be represented by the geometry in which a point source is placed at $\mathbf{r}'$ in front of the specimen and a thin lens is positioned after the specimen to splits the waves propagating along different directions (fig. 4(*a*)). Since the diffraction pattern is recorded at a large distance from the specimen, we can

Fig. 4

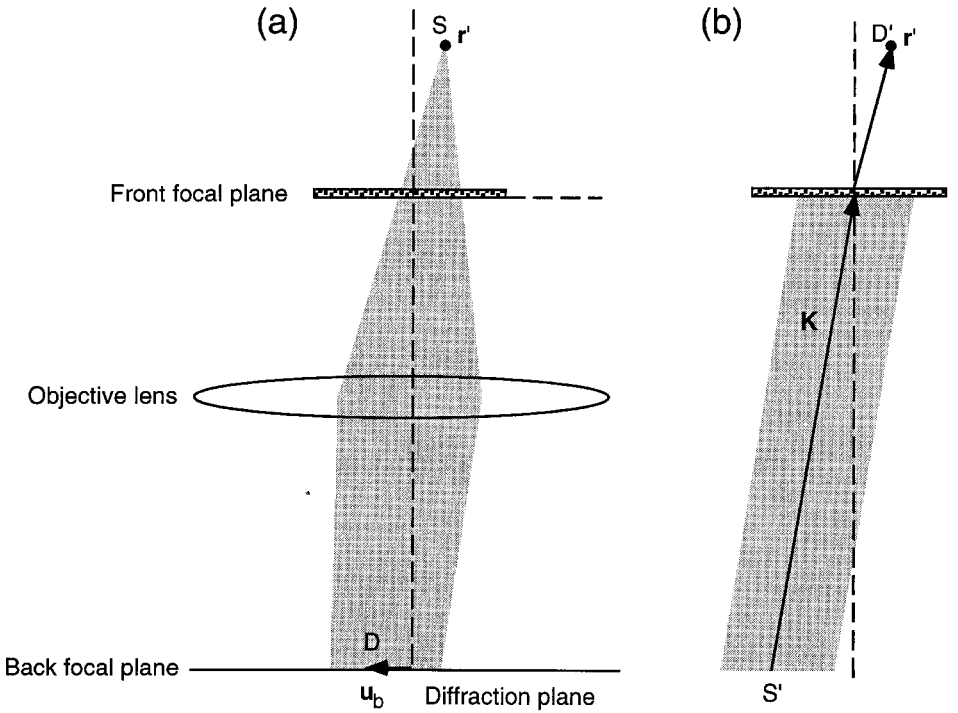

(*a*) Point-source electron diffraction in single-lens TEM. (*b*) An equivalent process based on the reciprocity theorem. The wavefunction observed at point $\mathbf{u}_b$ in reciprocal space due to a point source S at $\mathbf{r}'$ is equivalent to that observed at D′ arising from an incident plane wave with wave-vector $\mathbf{K} = -(\mathbf{u}_b, \kappa_z)$, striking the crystal from the bottom.

approximately take $z = \infty$, and the calculation is to find the distribution of the scattered electrons in reciprocal space, a mathematical description of this process is given below according to eqn. (9):

$$\hat{G}(\mathbf{u}_b, z, \mathbf{r}') = \int d\mathbf{b} \exp(-2\pi i \mathbf{u}_b \cdot \mathbf{b})\, G(\mathbf{b}, z, \mathbf{r}')$$

$$= \frac{C}{\pi} \int d\kappa_z \frac{\exp(2\pi i \kappa_z z)}{\kappa_z^2 + u_b^2 - K_0^2 - i0} \Psi_0^{(0)}(-\mathbf{u}_b, -\kappa_z, \mathbf{r}'), \qquad (22)$$

where $\mathbf{u}_b$ is a reciprocal-space vector parallel to the observation plane (x, y). Using an identity of

$$\frac{1}{x - x' - i0} = P\left(\frac{1}{x - x'}\right) + i\pi\delta(x - x'), \qquad (23)$$

where P signifies the principal value (i.e. the function $1/(x - x')$ is given as $1/(x - x')$ for all values of x' except at the point $x = x'$, for which $1/(x - x')$ is

taken to be identically zero), eqn. (22) becomes

$$\hat{G}(\mathbf{u}_b, z = \infty, \mathbf{r}') = \frac{C}{\pi}\int d\kappa_z \left[P\left(\frac{\exp(2\pi i\kappa_z z)}{\kappa_z^2 + u_b^2 - K_0^2}\right) + i\,\frac{\pi \exp(2\pi i\kappa_z z)}{2\kappa_z}\,\delta\left[\kappa_z - (K_0^2 - u_b^2)^{1/2}\right]\right] \Psi_0^{(0)}(-\mathbf{u}_b, -\kappa_z, \mathbf{r}')$$
$$= \frac{i m_0}{4\pi\hbar^2}\,\frac{\exp(2\pi i\kappa_z z)}{\kappa_z}\,\Psi_0^{(0)}(-\mathbf{u}_b, -\kappa_z, \mathbf{r}') \qquad (24)$$

where the first term vanishes because of the rapid oscillation of the exponential within the integral at large z, and $\kappa_z = (K_0^2 - u_b^2)^{1/2}$. This is the same result derived using an alternative technique (Dudarev *et al.* 1993). Therefore the diffraction amplitude at $\mathbf{u}_b$ is proportional to the electron wave scattered to $\mathbf{r}'$ arising from a plane-wave incidence with wave-vector $\mathbf{K} = -(\mathbf{u}_b, \kappa_z)$, where the negative sign represents the wave striking the crystal from the bottom side. This is again the result of the reciprocity theorem, as shown in fig. 4(*b*).

§ 4. Iterative calculation of the Green's function by the Born series

The calculation of the Green's function, in principle, can be carried out following eqn. (9), but the computation of this equation, however, could be huge because of the requirements of the elastic waves risen from a wide range of wave-vectors. In this section, we introduce the Born series technique for calculation of the Green's function. As stated in eqn. (5), the first term is the Green's function in free space and the second term is the kinematical scattering component of the Green's function. The nth term $\mathscr{g}_n(\mathbf{r}, \mathbf{r}')$ in eqn. (5) is related to the $(n-1)$th term $\mathscr{g}_{n-1}(\mathbf{r}, \mathbf{r}')$ by a recurrence formula

$$\mathscr{g}_n(\mathbf{r}, \mathbf{r}') = e\gamma \int d\mathbf{r}_1\, G_0(\mathbf{r}, \mathbf{r}_1)\, V_0(\mathbf{r}_1)\, \mathscr{g}_{n-1}(\mathbf{r}_1, \mathbf{r}'). \qquad (25)$$

For easy calculation, a double Fourier transform of $\mathscr{g}_n$ is taken:

$$\hat{\mathscr{g}}_n(\mathbf{u}, \mathbf{v}) = \int d\mathbf{r} \int d\mathbf{r}' \exp(-2\pi i \mathbf{u}\cdot\mathbf{r}) \exp(-2\pi i \mathbf{v}\cdot\mathbf{r}')\, \mathscr{g}_n(\mathbf{r}, \mathbf{r}')$$
$$= D\,\frac{1}{u^2 - K_0^2 - i0} \int d\mathbf{r}_1 \exp(-2\pi i \mathbf{u}\cdot\mathbf{r}_1)\, V_0(\mathbf{r}_1)\, \hat{\mathscr{g}}_{n-1}(\mathbf{r}_1, \mathbf{v})$$
$$= D\,\frac{1}{u^2 - K_0^2 - i0} \left[V_0(\mathbf{u}) \otimes \hat{\mathscr{g}}_{n-1}(\mathbf{u}, \mathbf{v}) \right], \qquad (26)$$

where $V_0(\mathbf{u})$ is the Fourier transform of the potential $V_0(\mathbf{r})$, and $D = (e\gamma m_0)/(2\pi^2\hbar^2)$. This relation clearly states that the nth-order term is a convolution of the crystal scattering factor with the $(n-1)$th-order term. This is a useful relationship for calculating the Green's function using mathematical induction. The 'average' potential V_0 is defined as a periodic function and it can be written as a Fourier series:

$$V_0(\mathbf{r}) = \sum_g V_g \exp(2\pi i \mathbf{g}\cdot\mathbf{r}) \quad \text{or} \quad V_0(\mathbf{u}) = \sum_g V_g \delta(\mathbf{u} - \mathbf{g}), \qquad (27)$$

where V_g are the so-called structure factors which are related to the atom types and

atom distribution in the unit cell. From eqn. (26),

$$\hat{\psi}_n(\mathbf{u},\mathbf{v}) = D\frac{1}{u^2 - K_0^2 - \mathrm{i}0}\sum_{g} V_g \hat{\psi}_{n-1}(\mathbf{u}-\mathbf{g},\mathbf{v}). \tag{28}$$

The zeroth order is

$$\hat{\psi}_0(\mathbf{u},\mathbf{v}) = \frac{C}{\pi}\frac{\delta(\mathbf{u}+\mathbf{v})}{v^2 - K_0^2 - \mathrm{i}0}, \tag{29}$$

from which the first order is calculated:

$$\hat{\psi}_1(\mathbf{u},\mathbf{v}) = \frac{CD}{\pi}\frac{1}{(u^2 - K_0^2 - \mathrm{i}0)(v^2 - K_0^2 - \mathrm{i}0)}\sum_{g_1} V_{g_1}\delta(\mathbf{u}+\mathbf{v}-\mathbf{g}_1). \tag{30}$$

A substitution of eqn. (30) into eqn. (28) gives the second-order term

$$\hat{\psi}_2(\mathbf{u},\mathbf{v}) = \frac{CD^2}{\pi}\frac{1}{(u^2 - K_0^2 - \mathrm{i}0)(v^2 - K_0^2 - \mathrm{i}0)}\sum_{g_1}\sum_{g_2}\frac{V_{g_1}V_{g_2}\delta(\mathbf{u}+\mathbf{v}-\mathbf{g}_1-\mathbf{g}_2)}{(|\mathbf{u}-\mathbf{g}_1|^2 - K_0^2 - \mathrm{i}0)}. \tag{31}$$

The third-order term is calculated accordingly:

$$\hat{\psi}_3(\mathbf{u},\mathbf{v}) = \frac{CD^n}{\pi}\frac{1}{(u^2 - K_0^2 - \mathrm{i}0)(v^2 - K_0^2 - \mathrm{i}0)} \times \sum_{g_1}\sum_{g_2}\sum_{g_3}\frac{V_{g_1}V_{g_2}V_{g_3}\delta(\mathbf{u}+\mathbf{v}-\mathbf{g}_1-\mathbf{g}_2-\mathbf{g}_3)}{(|\mathbf{u}-\mathbf{g}_1|^2 - K_0^2 - \mathrm{i}0)(|\mathbf{u}-\mathbf{g}_1-\mathbf{g}_2|^2 - K_0^2 - \mathrm{i}0)}. \tag{32}$$

For the higher-order terms with $n > 1$,

$$\begin{aligned}
\hat{\psi}_n(\mathbf{u},\mathbf{v}) = {} & \frac{CD^n}{\pi}\frac{1}{(u^2 - K_0^2 - \mathrm{i}0)(v^2 - K_0^2 - \mathrm{i}0)} \\
& \times \sum_{g_1}\cdots\sum_{g_n} V_{g_1}\cdots V_{g_n} \\
& \times \delta\left(\mathbf{u}+\mathbf{v}-\sum_n \mathbf{g}_n\right)\Big/(|\mathbf{u}-\mathbf{g}_1|^2 - K_0^2 - \mathrm{i}0)\cdots(|\mathbf{u}-\mathbf{g}_1-\cdots-\mathbf{g}_{n-1}|^2 - K_0^2 - \mathrm{i}0) \\
= {} & \frac{CD^n}{\pi}\left[P\left(\frac{1}{u^2 - K_0^2}\right) + \mathrm{i}\frac{\pi}{2K_0}\delta(u - K_0)\right]\left[P\left(\frac{1}{v^2 - K_0^2}\right) + \mathrm{i}\frac{\pi}{2K_0}\delta(v - K_0)\right] \\
& \times \left\{\sum_{g_1}\cdots\sum_{g_n} V_{g_1}\cdots V_{g_n}\delta\left(\mathbf{u}+\mathbf{v}-\sum_n \mathbf{g}_n\right)\left[P\left(\frac{1}{|\mathbf{u}-\mathbf{g}_1|^2 - K_0^2}\right)\right.\right. \\
& \left. + \mathrm{i}\frac{\pi}{2K_0}\delta(|\mathbf{u}-\mathbf{g}_1| - K_0)\right] \\
& \times \cdots\left[P\left(\frac{1}{|\mathbf{u}-\mathbf{g}_1-\cdots-\mathbf{g}_{n-1}|^2 - K_0^2}\right)\right. \\
& \left.\left. + \mathrm{i}\frac{\pi}{2K_0}\delta(|\mathbf{u}-\mathbf{g}_1-\cdots-\mathbf{g}_{n-1}| - K_0)\right]\right\}.
\end{aligned} \tag{33}$$

These terms appear to have singularities while performing the integrals but, as will be shown in the next section, the integrals will be split into volume, surface, line and point integrals, in which the singularities are automatically resolved.

§ 5. Calculation of the optical potential

As derived in the paper by Wang (1996c), dynamic multiple diffuse scattering introduced by point defects (with or without short-range order) and thermal diffuse scattering can be included in the calculation with introduction of a complex optical potential. This potential is a non-local function and it is best presented in the matrix form

$$V_{gh}^{(i)} = \frac{e\gamma}{V_c}\int d\mathbf{Q}\int d\mathbf{Q}' S(\mathbf{Q},\mathbf{Q}')\hat{G}(\mathbf{k}_i + \mathbf{g} - \mathbf{Q}, \mathbf{Q}' - \mathbf{k}_i - \mathbf{h}), \tag{34}$$

where S is the dynamic form factor for the diffuse scattering (Wang 1995b, 1996a), $\mathbf{g}$ and $\mathbf{h}$ are reciprocal-lattice vectors, $\mathbf{k}_i$ is the electron wave-vector in the Bloch wave representation, V_c is the volume of the crystal, and the integrations of $\mathbf{Q}$ and $\mathbf{Q}'$ cover the entire reciprocal space. In all the current dynamic calculations, the optical potential takes the form in which the Green's function is approximated by its form in free space as first introduced by Yoshioka (1957). We now use the first-order approximation to illustrate the consequence of including the crystal potential in the calculation of the optical potential V'. If only the first two terms are kept for the Green's function, the double Fourier transform of G is

$$\hat{G}(\mathbf{u},\mathbf{v}) \approx \frac{C}{\pi}\frac{\delta(\mathbf{u}+\mathbf{v})}{v^2 - K_0^2 - i0} + \frac{CD}{\pi}\left(\sum_{g_1} V_{g_1}\delta(\mathbf{u}+\mathbf{v}-\mathbf{g}_1)\right)\Big/ (u^2 - K_0^2 - i0)(v^2 - K_0^2 - i0); \tag{35}$$

the optical potential given in eqn. (34) is

$$\begin{aligned} V_{gh}^{(i)} &\approx \frac{e\gamma C}{\pi V_c}\int d\mathbf{Q}\int d\mathbf{Q}' \frac{S(\mathbf{Q},\mathbf{Q}')}{|\mathbf{k}_i + \mathbf{g} - \mathbf{Q}|^2 - K_0^2 - i0}\left[\delta(\mathbf{Q}' - \mathbf{Q} + \mathbf{g} - \mathbf{h}) \right.\\ &\quad \left. + D\left(\sum_{g_1} V_{g_1}\delta(\mathbf{Q}' - \mathbf{Q} + \mathbf{g} - \mathbf{h} - \mathbf{g}_1)\right)\Big/ (|\mathbf{Q}' - \mathbf{k}_i - \mathbf{h}|^2 - K_0^2 - i0)\right]\\ &= \frac{e\gamma C}{\pi V_c}\int d\mathbf{u}\int d\mathbf{v}\,\frac{S(\mathbf{k}_i + \mathbf{g} - \mathbf{u}, \mathbf{v} + \mathbf{k}_i + \mathbf{h})}{u^2 - K_0^2 - i0}\\ &\quad \times\left[\delta(\mathbf{u}+\mathbf{v}) + D\left(\sum_{g_1} V_{g_1}\delta(\mathbf{u}+\mathbf{v}-\mathbf{g}_1)\right)\Big/ (v^2 - K_0^2 - i0)\right]\\ &= \frac{e\gamma C}{\pi V_c}\int d\mathbf{u}\left[\frac{S(\mathbf{k}_i + \mathbf{g} - \mathbf{u}, \mathbf{k}_i + \mathbf{h} - \mathbf{u})}{u^2 - K_0^2 - i0}\right.\\ &\quad \left. + D\sum_{g_1} V_{g_1}\frac{S(\mathbf{k}_i + \mathbf{g} - \mathbf{u}, \mathbf{k}_i + \mathbf{h} - \mathbf{u} + \mathbf{g}_1)}{(u^2 - K_0^2 - i0)(|\mathbf{u} - \mathbf{g}_1|^2 - K_0^2 - i0)}\right] \end{aligned}$$

$$= \frac{e\gamma C}{\pi V_c}\left[\int d\tau(\mathbf{u})\,\frac{S(\mathbf{k}_i+\mathbf{g}-\mathbf{u},\mathbf{k}_i+\mathbf{h}-\mathbf{u})}{u^2-K_0^2} + i\frac{\pi}{2K_0}\int d\sigma(\mathbf{u})\,S(\mathbf{k}_i+\mathbf{g}-\mathbf{u},\mathbf{k}_i+\mathbf{h}-\mathbf{u})\right] + \frac{e\gamma CD}{\pi V_c}\sum_{g_1} V_{g_1}\left[\int d\tau'(\mathbf{u})\,\frac{S(\mathbf{k}_i+\mathbf{g}-\mathbf{u},\mathbf{k}_i+\mathbf{h}-\mathbf{u}+\mathbf{g}_1)}{(u^2-K_0^2)(|\mathbf{u}-\mathbf{g}_1|^2-K_0^2)} + i\frac{\pi}{2K_0}\int d\sigma'(\mathbf{u})\,\frac{S(\mathbf{k}_i+\mathbf{g}-\mathbf{u},\mathbf{k}_i+\mathbf{h}-\mathbf{u}+\mathbf{g}_1)}{|\mathbf{u}-\mathbf{g}_1|^2-K_0^2} + i\frac{\pi}{2K_0}\int d\sigma'(\mathbf{u}-\mathbf{g}_1)\,\frac{S(\mathbf{k}_i+\mathbf{g}-\mathbf{u},\mathbf{k}_i+\mathbf{h}-\mathbf{u}+\mathbf{g}_1)}{u^2-K_0^2} - \pi^2\int d\sigma''(\mathbf{u})\,S(\mathbf{k}_i+\mathbf{g}-\mathbf{u},\mathbf{k}_i+\mathbf{h}-\mathbf{u}+\mathbf{g}_1)\delta(|\mathbf{u}-\mathbf{g}_1|-K_0)\right], \quad (36)$$

where the terms in the first large square brackets are those first derived by Yoshioka (1957) when the Green's function if replaced by its form in free space; the terms contained in the second large square brackets are those from the first-order kinematical electron diffraction as included in the Green's function calculation; the integral $\tau'(\mathbf{u})$ is over all reciprocal space except for the spherical shells defined by $|\mathbf{u}| = K_0$ and $|\mathbf{u}-\mathbf{g}_1| = K_0$, the two Ewald spheres centred at $\mathbf{u}=\mathbf{0}$ and $\mathbf{u}=\mathbf{g}$ (fig. 5(*a*)); the integral $\sigma'(\mathbf{u})$ is over the Ewald sphere surface defined by $|\mathbf{u}| = K_0$ except for points falling on the other Ewald sphere defined by $|\mathbf{u}-\mathbf{g}_1| = K_0$; the integral $\sigma'(\mathbf{u}-\mathbf{g}_1)$ is over the Ewald sphere surface defined by $|\mathbf{u}-\mathbf{g}_1| = K_0$ except for the points intersecting the other Ewald sphere defined by $|\mathbf{u}| = K_0$; the last integral $\sigma''(\mathbf{u})$ covers the intersection lines of the two Ewald spheres (i.e. a line integral). The volume and line integrals give a real component correction to the potential; the surface integrals give an imaginary component which is usually referred to as the absorption potential. Since the calculation includes the first-order diffraction effect in the Green's function, the Ewald sphere $|\mathbf{u}-\mathbf{g}_1| = K_0$ represents the newly generated scattering centre at $\mathbf{g}_1$ due to Bragg reflection. The sum over $\mathbf{g}_1$ is to consider the contributions from all the possible Bragg reflections scaled kinematically by the structure factor V_{g_1}.

The number of spheres involved in each calculation depends on the order of scattering to be included in the Green's function calculation. For higher-order scattering, the integral of points characterized by delta functions (such as the joint points of three spheres) is possible, as shown in fig. 5(*b*) for the second-order scattering. The split of the integrals into volume, surface and line integrals automatically resolve the singularity problem in the calculation. Further, the function $1/(u^2-K_0^2)$ is an asymmetric function when $u \to K_0 + 0$ and $u \to K_0 - 0$; thus the integral is close to zero around $u = K_0$.

§ 6. Conclusion

In this paper we have introduced the properties and solution of the Green's function for electron scattering in a general scattering geometry for both high- and low-energy electrons. The theory has been extended into the regimes that are suitable for numerical calculations in different scattering geometry, such as the low-voltage lensless point-projection microscopy. The image calculation is equivalent to

Fig. 5

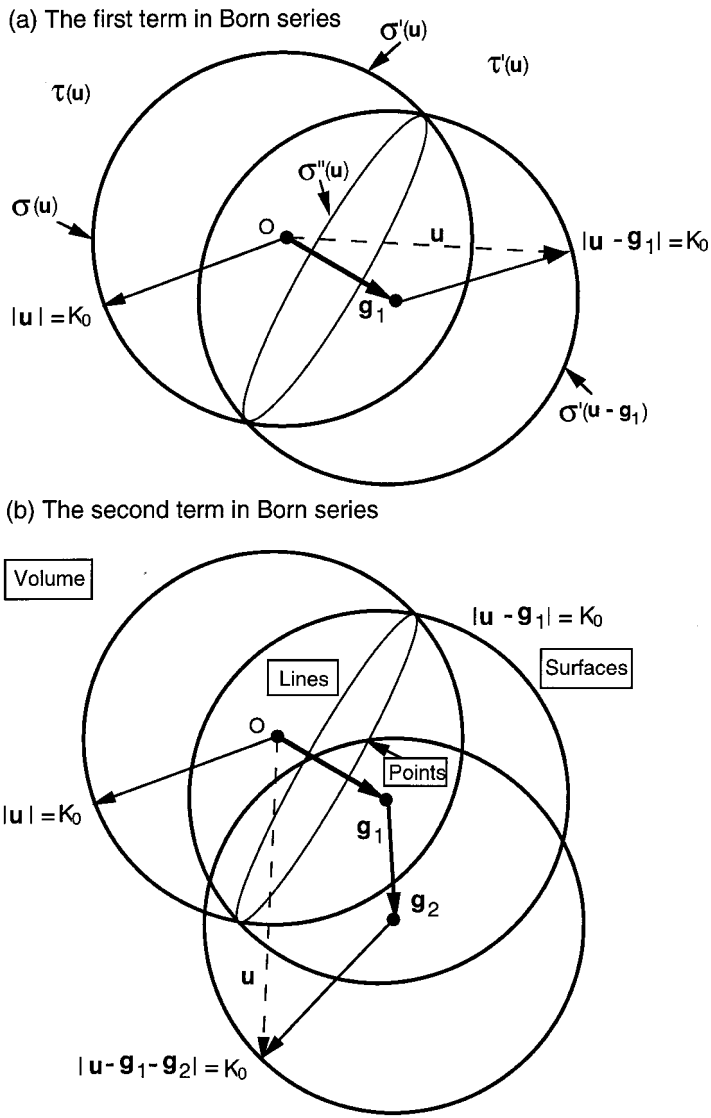

(*a*) A model of two interpenetrating Ewald spheres centred at $\mathbf{u} = 0$ and $\mathbf{u} = \mathbf{g}$ respectively, showing the volume, surface and line integrals introduced in eqn. (36). (*b*) A model for three interpenetrating Ewald spheres illustrating the occurrence of point integral (e.g. the integral of the delta function).

the simulation of on-axis bright-field shadow images in STEM when the incident electron probe is a plane wave.

An iterative calculation technique is introduced for computing the Green's function using the Born series, and the result has been applied to calculate the optical potential introduced in electron diffraction for recovering the multiple diffuse scattering effects that have been ignored in most of the current calculations. With the

Green's function presented here, the theory given in the previous paper (Wang 1996c) can be fully implemented numerically. This is likely to be a unique and full inclusion of the dynamic diffuse scattering arisen from short-range order of point defects and thermal diffuse scattering, providing the theoretical basis for quantifying experimental data. This is important for quantitative characterization and refinement of crystal structures with partially ordered point defects. This is foreseen with the current experimental feasibility of recording energy-filtered electron diffraction patterns and images.

APPENDIX

We now prove that the solution given by eqn. (9) satisfies $G(\mathbf{r},\mathbf{r}') = G(\mathbf{r}',\mathbf{r})$. Substituting eqn. (7) into eqn. (9), one has

$$\begin{aligned} G(\mathbf{r},\mathbf{r}') = \frac{m_0}{2\pi^2\hbar^2}\int \mathrm{d}\boldsymbol{\kappa}\,\frac{\exp(-2\pi\mathrm{i}\boldsymbol{\kappa}\cdot\mathbf{r}')}{\kappa^2 - K_0^2 - \mathrm{i}0}\Bigg(&\phi(\boldsymbol{\kappa},\mathbf{r}) + e\gamma\int \mathrm{d}\mathbf{r}_1\, G_0(\mathbf{r},\mathbf{r}_1)\,V_0(\mathbf{r}_1)\phi(\boldsymbol{\kappa},\mathbf{r}_1) \\ &+ (e\gamma)^2\int \mathrm{d}\mathbf{r}_1\int \mathrm{d}\mathbf{r}_2\, G_0(\mathbf{r},\mathbf{r}_1)G_0(\mathbf{r}_1,\mathbf{r}_2)\,V_0(\mathbf{r}_1)\,V_0(\mathbf{r}_2)\phi(\boldsymbol{\kappa},\mathbf{r}_2) \\ &+ (e\gamma)^3\int \mathrm{d}\mathbf{r}_1\int \mathrm{d}\mathbf{r}_2\int \mathrm{d}\mathbf{r}_3\, G_0(\mathbf{r},\mathbf{r}_1)G_0(\mathbf{r}_1,\mathbf{r}_2)G_0(\mathbf{r}_2,\mathbf{r}_3)\,V_0(\mathbf{r}_1)\,V_0(\mathbf{r}_2)\,V_0(\mathbf{r}_3)\phi(\boldsymbol{\kappa},\mathbf{r}_3) \\ &+ \cdots\Bigg). \end{aligned} \tag{A 1}$$

Integrating over $\boldsymbol{\kappa}$ and using eqn. (10 *a*) yield

$$\begin{aligned} G(\mathbf{r},\mathbf{r}') = {} & G_0(\mathbf{r},\mathbf{r}') + e\gamma\int \mathrm{d}\mathbf{r}_1\, G_0(\mathbf{r},\mathbf{r}_1)\,V_0(\mathbf{r}_1)G_0(\mathbf{r}_1,\mathbf{r}') \\ &+ (e\gamma)^2\int \mathrm{d}\mathbf{r}_1\int \mathrm{d}\mathbf{r}_2\, G_0(\mathbf{r},\mathbf{r}_1)G_0(\mathbf{r}_1,\mathbf{r}_2)\,V_0(\mathbf{r}_1)\,V_0(\mathbf{r}_2)G_0(\mathbf{r}_2,\mathbf{r}') \\ &+ (e\gamma)^3\int \mathrm{d}\mathbf{r}_1\int \mathrm{d}\mathbf{r}_2\int \mathrm{d}\mathbf{r}_3\, G_0(\mathbf{r},\mathbf{r}_1)G_0(\mathbf{r}_1,\mathbf{r}_2)G_0(\mathbf{r}_2,\mathbf{r}_3) \\ &\times V_0(\mathbf{r}_1)\,V_0(\mathbf{r}_2)\,V_0(\mathbf{r}_3)G_0(\mathbf{r}_3,\mathbf{r}') + \cdots. \end{aligned} \tag{A 2}$$

Since $G_0(\mathbf{r},\mathbf{r}') = G_0(\mathbf{r}',\mathbf{r})$, exchanging the positions of the G_0 functions and the sequence of V_0 values and through variable substitution lead to

$$\begin{aligned} G(\mathbf{r},\mathbf{r}') = {} & G_0(\mathbf{r}',\mathbf{r}) + e\gamma\int \mathrm{d}\mathbf{r}_1\, G_0(\mathbf{r}',\mathbf{r}_1)\,V_0(\mathbf{r}_1)G_0(\mathbf{r}_1,\mathbf{r}) \\ &+ (e\gamma)^2\int \mathrm{d}\mathbf{r}_1\int \mathrm{d}\mathbf{r}_2\, G_0(\mathbf{r}',\mathbf{r}_1)G_0(\mathbf{r}_1,\mathbf{r}_2)\,V_0(\mathbf{r}_1)\,V_0(\mathbf{r}_2)G_0(\mathbf{r}_2,\mathbf{r}) \\ &+ (e\gamma)^3\int \mathrm{d}\mathbf{r}_1\int \mathrm{d}\mathbf{r}_2\int \mathrm{d}\mathbf{r}_3\, G_0(\mathbf{r}',\mathbf{r}_1)G_0(\mathbf{r}_1,\mathbf{r}_2)G_0(\mathbf{r}_2,\mathbf{r}_3) \\ &+ V_0(\mathbf{r}_1)\,V_0(\mathbf{r}_2)\,V_0(\mathbf{r}_3)G_0(\mathbf{r}_3,\mathbf{r}) + \cdots \\ = {} & G(\mathbf{r}',\mathbf{r}) \end{aligned} \tag{A 3}$$

which is the well known reciprocity theorem in optics.

If the positions of the point source and the observation point are translated by the same lattice vector $\mathbf{R}_m$ in a periodically structured crystal, for example $V_0(\mathbf{r} - \mathbf{R}_m) = V_0(\mathbf{r})$, the corresponding Green's function is

$$\begin{aligned} G(\mathbf{r} - \mathbf{R}_m, \mathbf{r}' - \mathbf{R}_m) = {} & G_0(\mathbf{r} - \mathbf{R}_m, \mathbf{r}' - \mathbf{R}_m) + e\gamma \int d\mathbf{r}_1\, G_0(\mathbf{r} - \mathbf{R}_m, \mathbf{r}_1)\, V_0(\mathbf{r}_1)\, G_0(\mathbf{r}_1, \mathbf{r}' - \mathbf{R}_m) \\ & + (e\gamma)^2 \int d\mathbf{r}_1 \int d\mathbf{r}_2\, G_0(\mathbf{r} - \mathbf{R}_m, \mathbf{r}_1)\, G_0(\mathbf{r}_1, \mathbf{r}_2) \\ & \times V_0(\mathbf{r}_1)\, V_0(\mathbf{r}_2)\, G_0(\mathbf{r}_2, \mathbf{r}' - \mathbf{R}_m) \\ & + (e\gamma)^3 \int d\mathbf{r}_1 \int d\mathbf{r}_2 \int d\mathbf{r}_3\, G_0(\mathbf{r} - \mathbf{R}_m, \mathbf{r}_1)\, G_0(\mathbf{r}_1, \mathbf{r}_2)\, G_0(\mathbf{r}_2, \mathbf{r}_3) \\ & \times V_0(\mathbf{r}_1)\, V_0(\mathbf{r}_2)\, V_0(\mathbf{r}_3)\, G_0(\mathbf{r}_3, \mathbf{r}' - \mathbf{R}_m) + \cdots . \end{aligned} \tag{A 4}$$

Since $G_0(\mathbf{r} - \mathbf{R}_m, \mathbf{r}' - \mathbf{R}_m) = G_0(\mathbf{r}, \mathbf{r}')$, a variable substitution of $\mathbf{r}_i$ by $\mathbf{r}_i - \mathbf{R}_m$ gives

$$G(\mathbf{r} - \mathbf{R}_m, \mathbf{r}' - \mathbf{R}_m) = G(\mathbf{r}, \mathbf{r}'). \tag{A 5}$$

Therefore the same wavefunction is observed if the source and the observation point are displaced by the same lattice vector, provided that the crystal is periodic and infinitely large.

Acknowledgement

This work was supported in part by National Science Foundation grant No. DMR-9632823.

References

Abrikosov, A. A., Gorkov, L. P., and Dzyaloshinskii, 1966, *Methods of Quantum Field Theory in Statistical Physics* (Englewood Cliffs, New Jersey: Prentice-Hall).

Cowley, J. M., 1995, *Diffraction Physics*, third edition (Amsterdam: North-Holland), chap. 1.

Dudarev, S. L., Peng, L. M., and Whelan, M. J., 1993, *Phys. Rev.* B, **48**, 13408.

Dudarev, S. L., Vvedensky, D. D., and Whelan, M. J., 1994, *Phys. Rev.* B, **50**, 14525.

Fink, H. W., Schmid, H., Kreuzer, H., and Wierzbicki, A., 1991, *Phys. Rev. Lett.*, **67**, 1543.

Humphreys, C. J., 1979, *Rep. Prog. Phys.*, **42**, 1826.

Ishizuka, K., 1982, *Acta crystallogr.* A, **38**, 773.

Kreuzer, H. J., Nakamura, K., Wierzbicki, A., Fink, H. W., and Schmid, H., 1992, *Ultramicroscopy*, **45**, 381.

Qian, W., Spence, J. C. H., and Zuo, J. M., 1993, *Acta crystallogr.* A, **49**, 436.

Spence, J. C. H., 1992, *Optik*, **92**, 57.

Spence, J. C. H., and Qian, W., 1992, *Phys. Rev.* B, **45**, 10271.

Spence, J. C. H., Qian, W., and Melmed, A. J., 1993, *Ultramicroscopy*, **52**, 473.

Spence, J. C. H., Qian, W., and Silveman, M. P., 1994, *J. Vac. Sci. Technol.* A, **12**, 542.

Spence, J. C. H., and Zuo, J. M., 1992, *Electron Microdiffraction* (New York: Plenum).

Tsvelik, A. M., 1995, *Quantum Field Theory in Condensed Matter Physics* (Cambridge University Press).

Wang, Z. L., 1995a, *Elastic and Inelastic Scattering in Electron Diffraction and Imaging* (New York: Plenum); 1995b, *Acta crystallogr.* A, **51**, 569; 1996a, *ibid.*, **52**, 717; 1996b, *Surf. Sci.*, **366**, 377†; 1996c, *Phil. Mag.* B, **74**, 733†.

Yoshioka, H., 1957, *J. phys. Soc. Japan*, **12**, 618.

† Equation (15) in Wang (1996c) and eqn. (16*b*) in Wang (1996b) contain typographical errors. The correct form of the equations should be

$$\langle |\Phi_0(\mathbf{K}_0, \mathbf{u}_b, t)|^2 \rangle_{ts} \approx |\langle \Phi_0(\mathbf{K}_0, \mathbf{u}_b, t) \rangle_{ts}|^2.$$